University of Groningen

Ultralight Ultrafast Enzymes

Zhang, Xuepei; Meng, Zhaowei; Beusch, Christian M.; Gharibi, Hassan; Cheng, Qing; Lyu, Hezheng; Di Stefano, Luciano; Wang, Jijing; Saei, Amir A.; Végvári, Ákos

Published in:
Angewandte Chemie - International Edition

IMPORTANT NOTE: You are advised to consult the publisher's version (publisher's PDF) if you wish to cite from it. Please check the document version below.

Document Version
Publisher's PDF, also known as Version of record

Publication date:
2024

Link to publication in University of Groningen/UMCG research database

GDCh

Research Articles

Angewandte
Chemie
International Edition
www.angewandte.org

Enzymes

Ultralight Ultrafast Enzymes**

Xuepei Zhang, Zhaowei Meng, Christian M. Beusch⁺, Hassan Gharibi⁺, Qing Cheng,
Hezheng Lyu, Luciano Di Stefano, Jijing Wang, Amir A. Saei, Ákos Végvári,
Massimiliano Gaetani, and Roman A. Zubarev*

Abstract: Inorganic materials depleted of heavy stable isotopes are known to deviate strongly in some physicochemical properties from their isotopically natural counterparts. Here we explored for the first time the effect of simultaneous depletion of the heavy carbon, hydrogen, oxygen and nitrogen isotopes on the bacterium *E. coli* and the enzymes expressed in it. Bacteria showed faster growth, with most proteins exhibiting higher thermal stability, while for recombinant enzymes expressed in depleted media, faster kinetics was discovered. At room temperature, luciferase, thioredoxin and dihydrofolate reductase and Pfu DNA polymerase showed up to a 250% increase in activity compared to the native counterparts, with an additional ~50% increase at 10°C. Diminished conformational and vibrational entropy is hypothesized to be the cause of the accelerated kinetics. Ultralight enzymes may find an application where extreme reaction rates are required.

Introduction

The question to what extent the isotopic composition of molecules plays a role in physical, chemical and biological processes has interested scientists since the discovery of stable isotopes by Aston in 1919. To answer this question best, pure isotopes of different elements have been isolated and studied. In solid state physics, it has been found that near-monoisotopic materials possess strongly deviating properties: e.g., silicon ^{28}Si (99.87%) has a 60% higher thermal conductivity at 80 K than silicon with natural ($\approx$92% ^{28}Si) isotopic composition.[1] Qualitatively similar results have been obtained for monoisotopic diamond (99.8% ^{12}C)[2] and gallium arsenide. Strikingly, the thermal conductivity of germanium enriched to 99.99% ^{70}Ge increased up to 8 times compared to the natural isotopic composition, in which the share of ^{70}Ge among the five stable germanium isotopes is 21.2%.[3] Today, monoisotopic ^{28}Si that is free of nuclear spins causing decoherence in a quantum system emerges as a critical material in the development of quantum information devices, such as quantum computers.[3]

On the molecular level, monoisotopic species can exhibit different kinetics of formation than their polyisotopic counterparts. In the reaction of ozone O_3 synthesis from molecular oxygen O_2 by electrical discharge, the isotope effects alter the reaction rates by typically 10% to 20% depending on the pressure and temperature of the gas in which ozone is formed.[4] The strictly monoisotopic isotopomers $^{16}O^{16}O^{16}O$, $^{17}O^{17}O^{17}O$ and $^{18}O^{18}O^{18}O$ have been

[*] X. Zhang, Z. Meng, C. M. Beusch,⁺ H. Gharibi,⁺ H. Lyu,
L. Di Stefano, J. Wang, A. A. Saei, Á. Végvári, M. Gaetani,
R. A. Zubarev
Division of Chemistry I, Department of Medical Biochemistry and
Biophysics, Karolinska Institutet
17177 Stockholm (Sweden)
E-mail: Roman.Zubarev@ki.se

Q. Cheng
Division of Biochemistry, Department of Medical Biochemistry and
Biophysics, Karolinska Institutet
17177 Stockholm (Sweden)

L. Di Stefano
European Research Institute for the Biology of Aging, University
Medical Center Groningen, University of Groningen (The Netherlands)

A. A. Saei
Department of Cell Biology, Harvard Medical School
Boston, MA (USA)

M. Gaetani
Chemical Proteomics Core Facility, Department of Medical Biochemistry and Biophysics, Karolinska Institute
17177 Stockholm (Sweden)

and
Chemical Proteomics, Science for Life Laboratory (SciLifeLab)
17177 Stockholm (Sweden)

R. A. Zubarev
＞Department of Pharmacological & Technological Chemistry, I.M.
Sechenov First Moscow State Medical University
119146 Moscow (Russia)
and
The National Medical Research Center for Endocrinology
Moskva, 115478 Moscow (Russia)

[⁺] These authors contributed equally to this work.

found to strongly deviate in formation kinetics from other isotopomers, especially from the tri-isotopic $^{16}O^{17}O^{18}O$.[5]

In biological systems, each of the four most abundant ele-ments (C, H, O and N) has more than one stable isotope, the lighter one being the most abundant (e.g., the share of ^{12}C is 98.9%). Microbes, plants and animals, including mammals, can grow in an environment with significantly altered ratios of stable isotopes compared to natural, but the phenotype of the organisms can be significantly affected.[6] Katz et al., prominent researchers of isotopic effects in biology, concluded in 1960s that the "organisms of different isotopic compositions are actually different organisms, to the degree that their isotopic compositions are removed from naturally occurring compositions".[6d]

Among the studies in which the heavy isotopes have been depleted, many reported effects relate to deuterium depletion in water. A major deuterium-depleted water (DDW) phenomenon is the depressed growth of cancer cells,[7] which is currently being exploited in a clinical trial.[8] Previously, while studying the antiproliferation effect of DDW in human lung adenocarcinoma cells, we determined that DDW induces mitochondrial redox imbalance that leads to oxidative stress.[9] In general, deuterium concentration between 80 ppm and 300 ppm (the natural value being ~150 ppm) is found to be a cell growth regulator.[10]

It is the easiest to manipulate the isotopic composition of bacteria and yeast, as some strains of these can grow on minimal media composed of water, inorganic salts and a simple organic compound (e.g., an amino acid, glucose or carboxylic acid) as a source of carbon. Most studies deal with enriched heavy isotopes, while simultaneous depletion of several heavy stable isotopes in growth media have been used for decades to produce near-monoisotopic bacterial proteins for structural studies, e.g. with high-resolution mass spectrometry.[11] Such proteins are lighter than the corresponding isotopically normal molecules (the latter are often designated as light molecules to differentiate them from those labelled with heavy isotopes) and thus the former are called ultralight herein. Unfortunately, in earlier literature no information on the growth rate in isotopically depleted media has been provided. As an exception, an enhanced growth of E. coli bacteria upon a 3-fold depletion of ^{13}C has been reported in our earlier work.[12]

Having acquired considerable experience in measuring the parameters of bacterial growth in various isotopic environments,[12–13] we decided to investigate the effect of the depleted media on the growth and phenotype of E. coli. For this, we formulated a M9 minimum media based on ^{13}C-depleted glucose and ^{15}N-depleted salt dissolved in D,^{18}O-depleted water (Depleted media). As a control, the growth of E. coli in isotopically natural media (Normal media) was monitored. Four different enzymes were recombinantly produced in Depleted as well as Normal media, and their activity was carefully measured. We report here on much bigger effects than previously found for isotopic phenomena in molecules as well as what could be expected for the replacement by light isotopes of only ~1% of all atoms.

Results and Discussion

The growth of E. coli BL21

The values of lag time, maximum growth rate and maximum density were used[21] for comparison of the E. coli growth in Normal and Depleted media (Figure 1A). All three parameters indicated that the Depleted media was more beneficial for bacterial growth, providing a significantly (all p-values ≪ 10^{-6}, $n = 21$) higher maximum density, faster growth rate as well as a shorter lag time (Figure 1B).

LC–MS analysis of bacterial lysate showed that in most proteins with MW < 20 kDa the monoisotopic mass dominates in the isotopic distribution of molecular ions (Figure 1C). Fourier Transform Isotopic Ratio Mass spectrometry (FT IsoR MS)[14] of the peptide digest obtained from E. coli lysate that is based on the analysis of the "fine structure" of fragment immonium ions of amino acid residues proved deep depletion of ^{13}C, significant depletion of ^{15}N as well as a moderate reduction in deuterium in bacterial proteins (Figure 1D).

Dose dependence in Depleted media dilution

When the Depleted media was diluted by the Normal media to below 80%, the maximum density of E. coli bacteria started to deviate significantly from that in pure Depleted media (Figure 1E), while maximum growth rate was affected only at a dilution below 40% (Figure S1A).

To test the effect of individual isotope depletion, we grew E. coli bacteria at the corresponding conditions, performing two independent experiments with $n = 16$ in each (Figure S1B). While depletion of ^{13}C gave on average an 8% growth boost, depletion of ^{15}N led to a 4% effect. On the other hand, using water depleted of both deuterium and ^{18}O gave a strong 18% growth enhancement. Simultaneous depletion of all heavy isotopes resulted in a 29% boost, which was close to the arithmetic sum of the individual effects (+30%), and thus no collective effect of multiple isotope depletion could be postulated.

Thermal stability of bacterial proteins

Thermal proteome profiling (TPP) is rapidly becoming a standard proteome analysis method.[15] Briefly, the cellular or bacterial lysate undergoes a 3 min incubation at a set of fixed temperature points ranging, e.g., from 37°C to 83°C, after which the denatured proteins that lost their solubility are spun down and the concentration of each remaining protein in the supernatant is measured by proteomics. The resultant data are fitted with a sigmoidal curve (Figure 2A), and the middle point provides the melting temperature Tm. When two conditions are compared, the difference △Tm is considered, interpreted as change in either thermal stability or solubility.

The distribution of E. coli △Tm values (Figure 2B, Supporting Information Table 1) reveals that more proteins
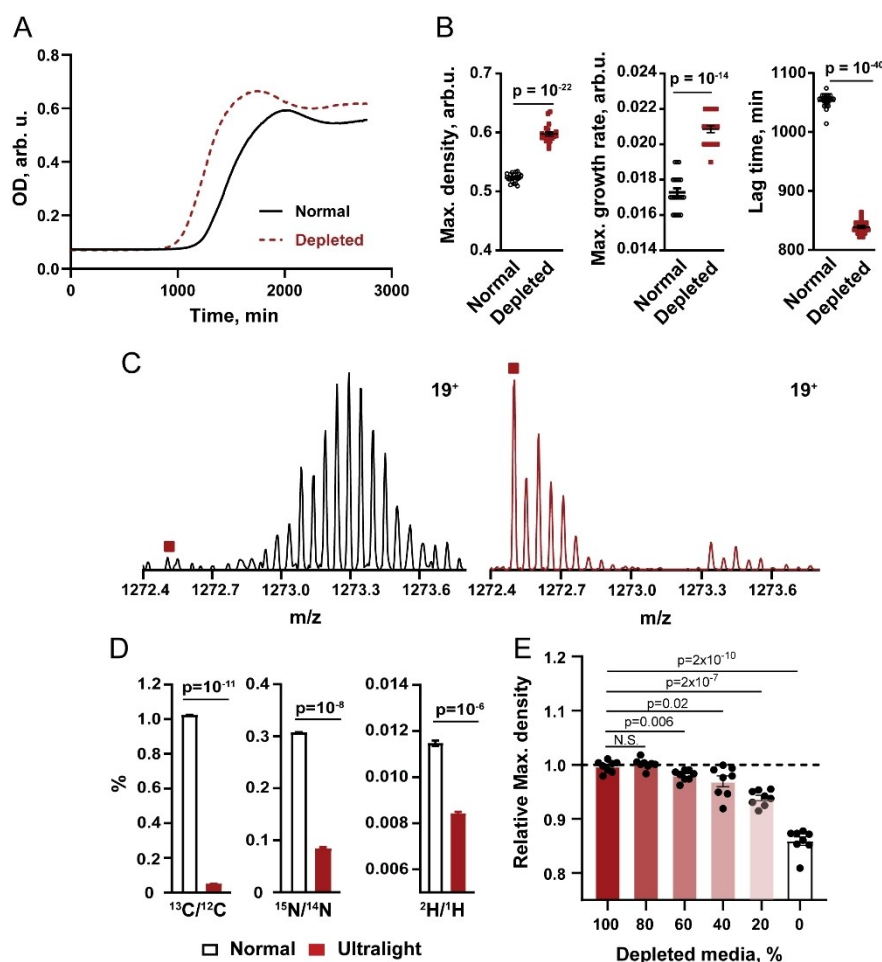
Figure 1. *E. coli* growth in Normal and Depleted media. (A) The growth curves of *E. coli* BL21 grown in Normal and Depleted M9 media ($n=21$). (B) The differences in maximum density (left), maximum growth rate (middle) and lag time (right) of *E. coli* grown in Normal and Depleted media ($n=21$). (C) Mass spectrum of the 19^+ molecular ion of *E. coli* Stringent Starvation Protein A (24.1 kDa) grown in the Normal (left) and Depleted (right) media. The monoisotopic mass position is marked by square. (D) FT isoR MS analysis of $^{13}C/^{12}C$ (left), $^{15}N/^{14}N$ (middle), $^{2}H/^{1}H$ (right) in *E. coli* grown in Normal and Depleted M9 media ($n=3$). (E) Dose-response effect of the Depleted media dilution by the Normal media on maximum density of *E. coli* bacteria ($n=8$). The plots show mean $\pm$ SEM of experiments. P values were calculated using two-tailed Student's t-test.

increase than decrease their thermal stability (or solubility) upon becoming ultralight. The median melting temperature of such proteins was $\triangle T_{m}=1.0\pm0.1\,°C$ higher than that of the proteins obtained in Normal media (Figure S2A). Pathway analysis of proteins becoming more (and less) soluble with temperature (Figure S2B–C) revealed that, e.g., translation-related proteins become less soluble with isotope depletion, while rRNA processing proteins become more soluble.

We also noticed that the melting curve of many Ultralight proteins shows steeper decline with temperature than their isotopically natural counterparts. To test this observation, the melting curves were fitted with the equation:

$$y = ((1\text{-}Pl)/(1 + \exp((T\text{-}Tm)/(B{*}T)))) + Pl \qquad (1)$$

where the term B is responsible for the slope steepness (lower values mean steeper curve) and Pl is the high-temperature plateau of the melting curve.[15–16] Of the 316

proteins found with significantly ($p < 0.05$) altered slope, 239 Ultralight proteins (76 %) had a steeper slope (Figure 2C, Supporting Information Table 2), with the median slope 27 % higher than that of their normal counterparts (Figure 2D).

Luciferase YY5

We expressed recombinantly luciferase YY5[17] in *E. coli* grown in both Normal and Depleted media. In order to ensure validity of the comparison, a single peak in size-exclusion chromatography (SEC) containing activity-possessing molecules was isolated (Figure S3A). However, mass spectrometry (MS) analysis showed that the peak contains at least two proteins with different molecular weights. Therefore, an additional purification step using strong cation exchange (SCX) chromatography was implemented, which gave two well-separated fractions, fracI and fracII (Fig-
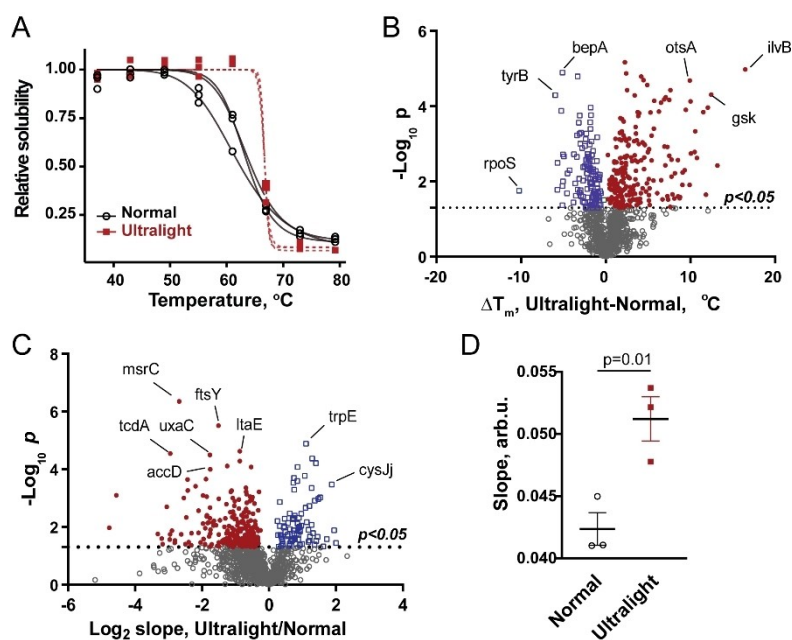
Figure 2. Thermal stability of bacterial proteins. (A) The melting curves of gltB in _E. coli_ BL21 grown in Normal and Depleted media ($n = 3$). (B) Volcano plot of melting temperature differences of proteins in _E. coli_ grown in Depleted versus Normal media (median values, $n = 3$). The horizontal line indicates the p value of 0.05 in two-tailed unpaired t-test. The proteins more stable in the Depleted media have positive $\triangle$Tm values (red dots), while less stable proteins have negative $\triangle$Tm values (blue dots). (C) Volcano plot of slopes of the _E. coli_ protein melting curves for bacteria grown in Depleted and Normal media (medians, $n = 3$). The horizontal line indicates the p value of 0.05 in two-tailed unpaired t-test. The proteins from the Depleted media with steeper slopes have negative Log$_2$ values (red dots), while those with more shallow slopes have positive values (blue dots). (D) Comparison of median slopes of proteins in _E. coli_ grown in Normal and Depleted media ($n = 3$). The plots show mean $\pm$ SEM of experiments. P values were calculated using two-tailed Student's t-test.

ure S2B). Both fractions, especially fracII, showed strong luciferase activity, and MS analysis confirmed that fracII contains only one molecular specie. Tandem MS analysis of that fraction provided isotopic distribution of the y_{87}^{12+} backbone fragment (12-times protonated C-terminal fragment containing 87 amino acid residues), with the mono-isotopic mass dominant in the Ultralight protein (Figure 3A). Charge deconvolution gave the average isotopic molecular mass (MW) of $61,728.9 \pm 0.3$ Da of the Normal luciferase in fracII, which was by 240.8 ± 0.3 Da higher than expected (Figure S3E). The difference was attributed to a combination of biotinylation and methylation, which are common post-translational modifications (PTMs) in recombinant proteins.[18] Bottom-up LC–MS/MS analysis of fracII digested with trypsin confirmed methylation at Lys-524 and biotinylation at Lys-329 (Figure S3I and J).

The Ultralight protein from fracII showed MW of $61,697.5 \pm 0.3$ Da, or 7.6 ± 0.4 Da higher than the expected monoisotopic mass including biotinylation and methylation (Figure S3E). Since in the normal sample, the theoretical difference between MW and monoisotopic masses (isotopic shift)[19] is 39.0 Da, the heavy isotopes in the Ultralight luciferase were depleted on average by 81 %:

$$\text{Depletion } [\%] = [\text{MW}_\text{Normal}\text{-MW}_\text{Ultralight})]/\text{Isotopic shift} \times 100\% \tag{2}$$

The activity of fraction fracII was measured for different concentrations of the substrate D-luciferin at 200 ng/mL enzyme concentration (Figure 3B). The fitted Michaelis–Menten equation provided the Vmax and Km values. The maximum reaction rate Vmax of the Ultralight luciferase was found to be 2.5 ± 0.2 higher than the normal one (p = 3×10^{-7}, $n = 4$), while the Km value (Michaelis constant, numerically equal to the substrate concentration at which the reaction rate is half of Vmax) was not significantly changed (Figure 3C). To test whether this result depended upon the enzyme concentration, we repeated the measurements at 40 ng/mL, with a similar outcome (Figure S3L). The activity of the Ultralight luciferase YY5 started to decline significantly when the Depleted media was diluted by the Normal media to below 80 % (Figure 3D), which was a similar effect to that observed for _E. coli_ growth parameters (Figure 1E).

The fraction fracI turned out to be heterogeneous, with the main component corresponding to a combination of double biotinylation and methylation (Figure S3C and 3D). This fraction showed an order of magnitude lower activity than fracII (Figure S3F and 3G). It also demonstrated a significant Ultralight/Normal ratio (termed here the acceleration factor) in maximum reaction rate (1.7 ± 0.2, p = 2×10^{-5}), and a small reduction in Km (0.87 ± 0.05, p = 0.02) (Figure S3H).

To test the refolding ability of the enzyme after thermal unfolding, the fracII luciferase samples were incubated at
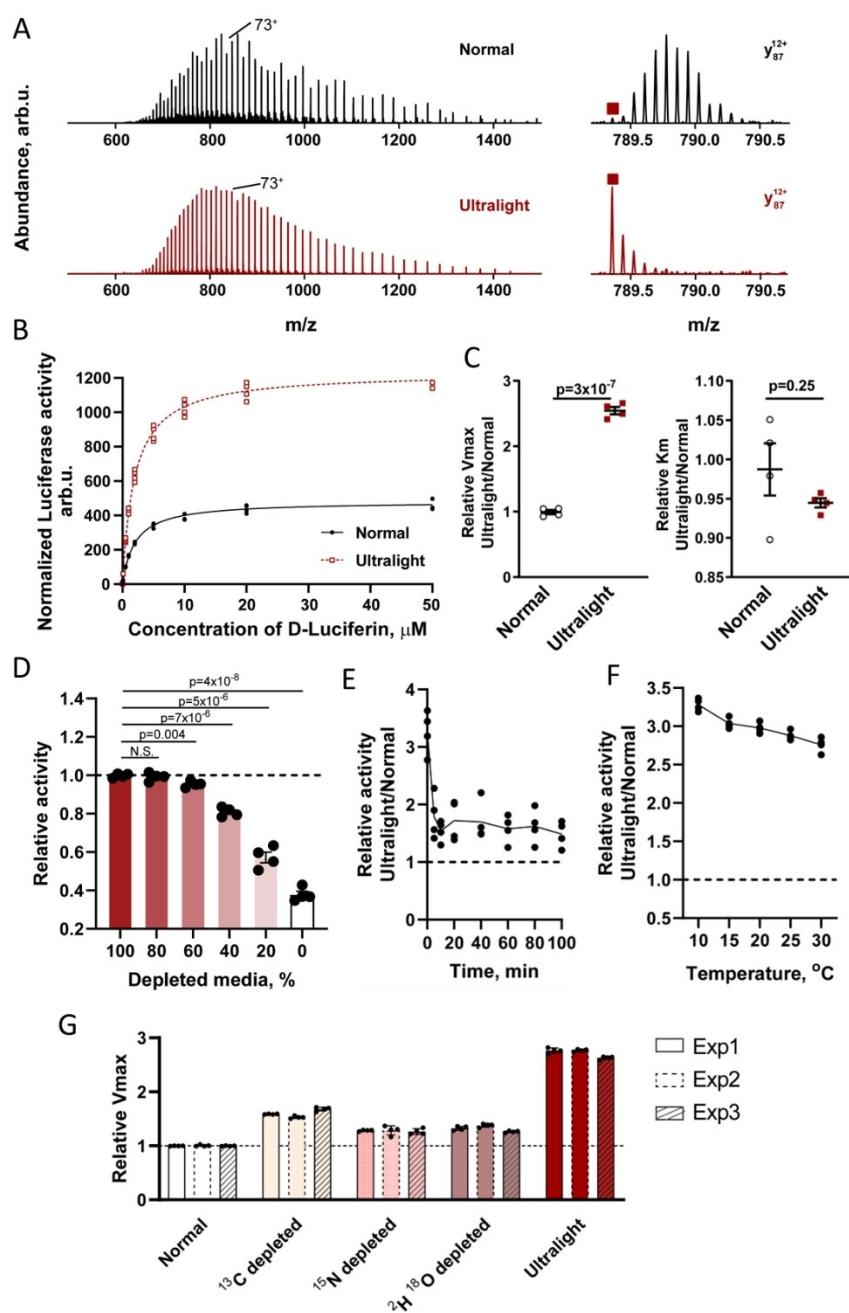
Figure 3. Analysis of luciferase YY5 fracII by mass spectrometry and activity comparison of Ultralight and Normal enzyme. (A) Electrospray ionization mass spectra of fracII of Normal and Ultralight luciferase YY5 with molecular ions in different charge states (73^+ is marked) (left) and a backbone fragment obtained by MS/MS of molecular ions; square denotes monoisotopic mass. (B) Activity curve of luciferase YY5 fracII. The luminescence readings ($n=4$) were normalized to the total UV absorbance in SCX chromatography before being fitted with the Michaelis–Menten equation. (C) Kinetic parameters Vmax (left) and Km (right) of the Normal and Ultralight luciferase YY5, fracII ($n=4$). (D) Dose-response effect of the Depleted media dilution by the Normal media on activity of Luciferase YY5 ($n=6$). (E) The relative activity of the Ultralight luciferase YY5 fracII compared to Normal enzyme after heating at 50°C for different time intervals and cooling to RT ($n=4$). (F) The relative activity of the Ultralight luciferase YY5 fracII compared to Normal enzyme at different temperatures ($n=4$). (G) Relative activity of luciferase YY5 fracII with individual isotope depletion ($n=12$ in three independent experiments). The plots show mean ± SEM of experiments. P values were calculated using two-tailed Student's t-test.

50°C for up to 100 min and then cooled down to RT. As expected, the enzyme activity has dropped, but at all tested time points, the Ultralight enzyme demonstrated a 1.6 ± 0.1 times higher activity than the normal enzyme (Figure 3E).

Importantly, at lowering temperature below RT the acceleration factor for untreated fracII enzyme was increasing, reaching 2.3 ± 0.1 at 10°C (Figure 3F). Nevertheless, thermal profiling showed that the Ultralight fracII luciferase had a

lower Tm by (0.6 ± 0.2) °C compared to the isotopically normal enzyme (Figure S3K).

Activity assay of luciferase YY5 fracII obtained with individual isotope depletion showed that ^{15}N depletion led to a 28% activity boost, while using (deuterium,[18]O)-depleted water increased the activity by 32% on average (Figure 3G). As expected, depletion of ^{13}C gave a stronger 62% activity enhancement (^{13}C is the main contributor to isotopic distribution of proteins). Remarkably, simultaneous depletion of all heavy isotopes resulted in a 151% boost, some 29% higher than the arithmetic sum of the individual isotope effects (+122%). This result may indicate the presence of a collective phenomenon for acceleration factor with isotopic depletion.

Melting curves showed that Ultralight luciferase YY5 fracII had a steeper slope and a significantly lower Tm (-0.64 ± 0.2°C, p=0.007, Figure S3K). Even at a 5 times lower enzyme concentration compared to that used in kinetic analysis, Ultralight luciferase YY5 fracII showed similarly higher activity compared with the Normal enzyme (Figure S3L).

Thioredoxin

Another tested enzyme was thioredoxin (Trx), an oxidation-reduction active enzyme containing a cystine disulfide that is reduced to the dithiol cysteine form by thioredoxin reductase (TrxR) with NADPH as a cofactor.[20] The reduced Trx can oxidize again by reducing its substrate, such as insulin that is composed of peptide chains A and B linked together by two disulfide bonds. Consumption of NADPH in solution results in the decrease of UV absorbance at 340 nm, which is used for measuring Trx activity. Trx (Figure S4A–C) was expressed recombinantly in *E. coli* grown in both Normal and Depleted media, purified and quantified by SEC (Figure S4D), with the purity verified by MS (Figure 4A). As expected, monoisotopic mass dominated in the isotopic distribution of molecular ions in the Ultralight sample (Figure S4E). The monoisotopic mass of the Ultralight protein was $11,784.9\pm0.1$ Da, which was by 1.9 ± 0.1 Da lower than expected. The difference was attributed to a disulfide linkage between two cysteine residues, which is a frequent post-translational modification in recombinant proteins.[21] The depletion of Ultralight Trx was determined to be 65%.

The activity of thioredoxin was measured in the presence of 200 µM NADPH. The decrease in 340 nm UV absorbance for the reaction catalyzed by Ultralight thioredoxin was significantly faster compared with the Normal enzyme (Figure 4B), which was reflected in a steeper decreasing curve for Ultralight thioredoxin. The kinetic curve of thioredoxin was measured for different concentrations of the substrate NADPH (Figure 4C) by fitting the Michaelis–Menten equation (Figure 4D). The maximum reaction rate of the Ultralight thioredoxin was found to be (17 ± 1)% higher than the Normal one (p=0.002, $n=3$), while the Km value was not significantly altered.

The activity of enzyme was also measured at different temperatures in the range 15–40°C. As expected, the enzyme activity dropped at lower temperature, but the Ultralight/Normal activity ratio increased to 2.0 ± 0.3 at 15°C (Figure 4E).

Dihydrofolate reductase

Dihydrofolate Reductase (DHFR) is a ubiquitous enzyme that is present in all eukaryotic and prokaryotic cells. DHFR catalyzes the transfer of a hydride from NADPH to dihydrofolate with an accompanying protonation to produce tetrahydrofolate, during which NADPH is oxidized to $NADP^+$. By monitoring the decrease in absorbance at 340 nm, a NADPH-specific wavelength, the ability of DHFR to catalyze the oxidation of NADPH can be measured.[22]

DHFR from *Geobacillus stearothermophilus* (BsDHFR, Figure S5A and 5B) was expressed recombinantly in *E. coli* grown in both Normal and Depleted media, purified and quantified by SEC (Figure S5C), with the purity verified by MS (Figure 5A). Monoisotopic mass dominates in the isotopic distribution of molecular ions in the Ultralight sample, while charge and isotope deconvolution of the Normal BsDHFR mass spectrum provided the average MW of 33820.4 ± 0.2, which was only 0.2 Da lower than expected and within the experimental error. The average mass of the Ultralight protein revealed the isotopic shift of only 5.0 ± 0.2 Da (Figure S5D), consistent with the depletion degree of 76%.

The activity of BsDHFR was measured in the presence of 200 µM DHF and 200 µM NADPH. The decrease in 340 nm UV absorbance for the reaction catalyzed by Ultralight BsDHFR was significantly faster compared with the Normal enzyme (Figure 5B). The activity of BsDHFR was measured for different concentrations (0–200 µM) of NADPH by fitting the Michaelis–Menten equation (Figure 5C), which revealed a (77 ± 6)% acceleration factor for the maximum reaction rate ($p=10^{-8}$, $n=8$), while the Km value was again not significantly changed.

Similar to other tested enzymes, the activity of BsDHFR measured in the range 10–30°C dropped at lower temperature, but the Ultralight/Normal activity ratio increased, reaching 2.1 ± 0.2 at 10°C (Figure 5E).

Methotrexate (MTX) is a well-known inhibitor of DHFR activity.[23] In TPP experiments, the melting temperature of DHFR-MTX complex is significantly increased compared to DHFR. To probe the △Tm difference for Normal and Ultralight DHFR, we mixed these two enzymes at a 1:1 ratio with and without added equimolar amounts of MTX. After 3 min incubation, the samples were ultra-centrifuged and the supernatant underwent trypsin digestion followed by FT IsoR MS analysis. Depletion of heavy C and N isotopes was found in DHFR incubated with MTX compared (Figure S4E), indicating higher Tm of the complex of Ultralight DHFR with MTX compared to the isotopically normal complex.
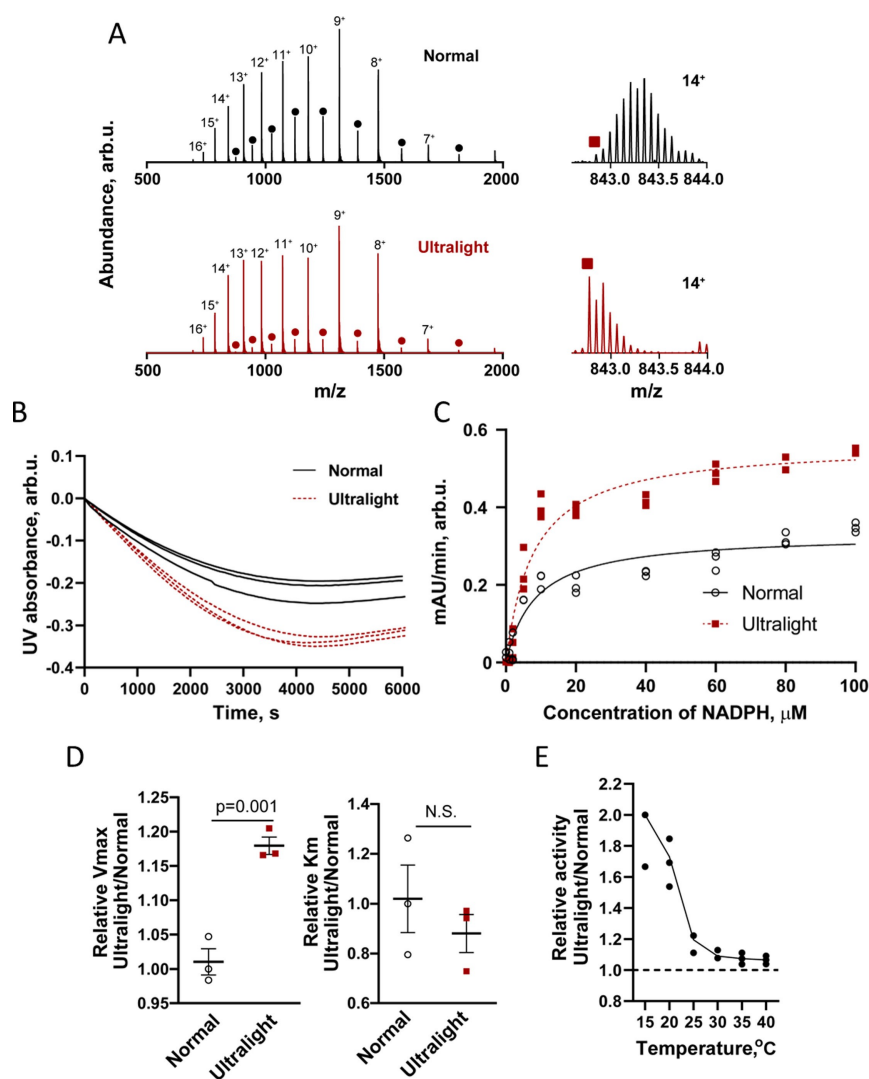
Figure 4. Analysis of Trx by mass spectrometry and activity comparison of Normal and Ultralight enzyme. (A) Electrospray ionization mass spectrum of the SEC-purified Normal (top) and Ultralight (bottom) thioredoxin. The dots indicate the thioredoxin dimer, squares - the monoisotopic masses (left). Isotopic distribution of the molecular ion in charge state 14^+ (right). (B) Activity comparison of Normal and Ultralight thioredoxin ($n=3$). (C) Kinetic curves of the Normal and Ultralight thioredoxin ($n=3$). (D) The kinetic parameters Vmax (left) and Km (right) of the Normal and Ultralight thioredoxin ($n=3$). (E) The relative activity of the Ultralight thioredoxin compared to Normal enzyme at different temperatures ($n=4$). The plots show mean $\pm$ SEM of experiments. P values were calculated using two-tailed Student's t-test.

Pfu DNA polymerase

Polymerase chain reaction (PCR) proved to be one of the biggest revolutions in molecular biology. Due to its extremely high sensitivity and dynamic range, the potential for high throughout as well as semi-quantitative nature, PCR is now widely used in research, clinical diagnostics, etc.[24] For example, viral nucleic acid detection by real time (RT)–PCR remains the gold standard of current diagnostic tests for the SARS-CoV-2 infection.[25] Although PCR is a mature technology, research is still ongoing to obtain more efficient and DNA polymerase less prone to sequence errors.[26] Pfu DNA polymerase[27] is a high-fidelity, thermo-stable enzyme isolated from *Pyrococcus furiosus.* In this study, Pfu DNA polymerase was expressed recombinantly in *E. coli* grown in both Normal and Depleted media, purified

and quantified by SEC (Figure S6A), with the purity verified by MS (Figure 6A). In the Ultralight sample, monoisotopic mass dominates in the isotopic distribution of $b_{99}{}^{20+}$ ions (20-times protonated dehydrated N-terminal fragment with 99 amino acid residues), which confirms strong depletion of heavy isotopes (Figure 6A). Charge deconvolution of the Normal Pfu DNA polymerase yielded the average MS of $100,194.3 \pm 0.6$, which was by 43.4 ± 0.6 Da higher than expected (Figure S6B). The difference was attributed to acetylation in combination with deamidation, which both are common PTMs in recombinant proteins.[18] The bottom-up LC–MS/MS analysis assigned the acetylation at His-21 and deamidation at Asn-757 (Figure S6C and 6D). Taking the mass shift into account, the Ultralight sample gave the isotopic shift of 12.1 ± 0.6 Da (Figure S6B), which corresponds to the depletion degree of 81 %.
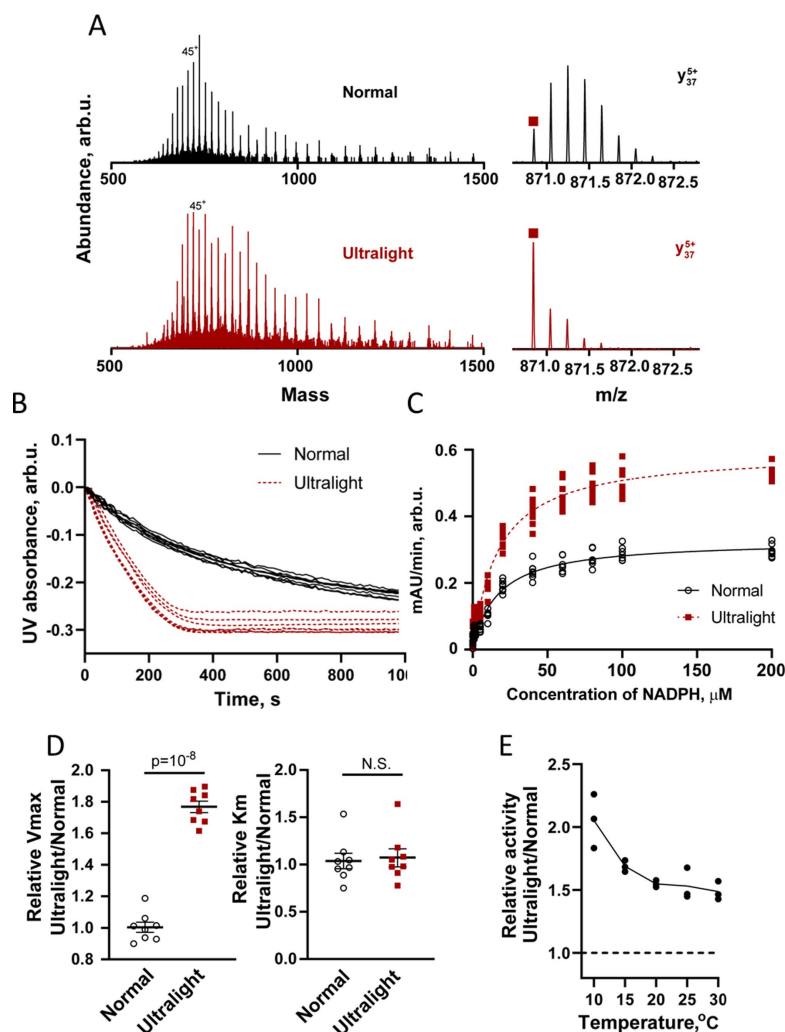
Figure 5. Analysis of BsDHFR by mass spectrometry and activity comparison of Normal and Ultralight enzyme. (A) Electrospray ionization mass spectra of Normal and Ultralight BsDHFR in different charge states (45^+ is marked) (left) and the isotopic distribution of the y_{37}^{5+} backbone fragment obtained by MS/MS of molecular ions; square - the monoisotopic mass. (B) Activity comparison of Normal and Ultralight BsDHFR ($n=8$). (C) Kinetic curves of the Normal and Ultralight BsDHFR ($n=8$). (D) The kinetic parameters Vmax (left) and Km (right) of the Normal and Ultralight BsDHFR ($n=8$). (E) The relative activity of the Ultralight BsDHFR compared to Normal enzyme at different temperatures ($n=3$). The plots show mean $\pm$ SEM of experiments. P values were calculated using two-tailed Student's t-test.

Human glyceraldehyde-3-phosphate dehydrogenase (GAPDH), one the most used reference genes in RT-PCR assays,[28] was selected as the targeted gene for activity assay. RNAs extracted from human non-small lung cancer cell line A549 cells was reverse transcribed to cDNAs which were used as templates for RT-PCR. With the concentration of input cDNAs 2 ng per 20 µL reaction it was found that RT-PCR catalyzed by Ultralight Pfu DNA polymerase was significantly faster compared to Normal enzyme (Figure 6B). The cycle threshold (Ct) value for RT-PCR (the number of cycles required for the fluorescent signal to cross the threshold) was 11.1 ± 0.3 cycles with Ultralight Pfu, while with Normal Pfu DNA polymerase it was 13.6 ± 0.4 cycles (Figure 6D), consistent with faster kinetics of the Ultralight enzyme. A qualitatively similar result was obtained at a lower concentration of cDNA (0.2 ng/20 µL reaction, Figure 6C), with Ct values 14.4 ± 0.4 cycles for Ultralight Pfu

DNA polymerase and 17.1 ± 0.3 cycles for the Normal enzyme (Figure 6E). The efficiency of PCR (the fraction of target molecules that are copied in one PCR cycle) with the Ultralight enzyme was significantly higher, $(97.7\pm0.8)\%$, compared to the Normal enzyme, $(92.8\pm2)\%$ (Figure 6F). Moreover, the amount of final product in the reaction with the Ultralight enzyme was higher than with the Normal enzyme (Figure S6E), which additionally supported the higher efficiency of Ultralight Pfu DNA polymerase.

The activity of the Pfu DNA polymerase at different extension temperatures in the range 60–72 °C was studied by detection of the fluorescence intensity of SYBR green I which presented the amount of double-stranded DNA (dsDNA) produced in PCR. As expected, the enzyme activity dropped at lower temperature (Figure S6E), but the acceleration factor increased, with a $(54\pm5)\%$ higher activity for Ultralight enzyme at 60 °C (Figure 6G).
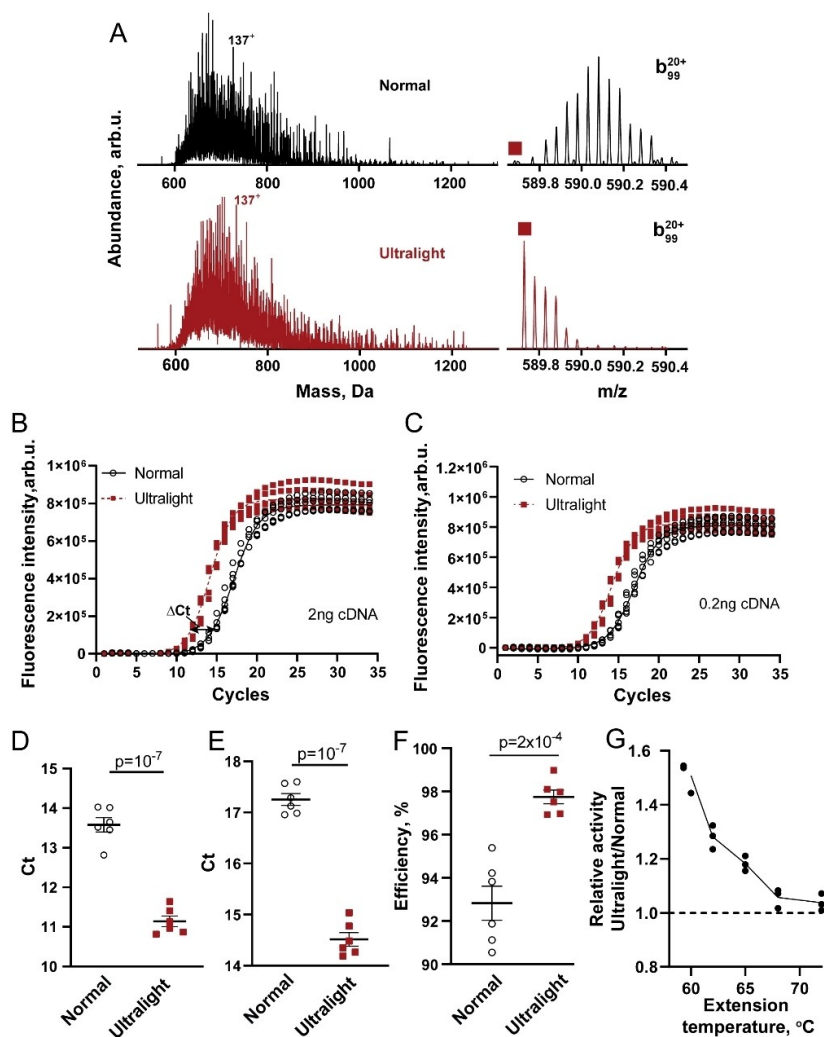
Figure 6. Analysis of Pfu DNA polymerase by mass spectrometry and activity comparison of Normal and Ultralight enzyme. (A) Electrospray ionization mass spectra from SEC of Normal and Ultralight Pfu DNA polymerase in different charge states (137^+ is marked) (left) and the isotopic distribution of the b_{99}^{20+} backbone fragment obtained by MS/MS of molecular ions; square - the monoisotopic mass. (B), (C), Comparisons of the RT PCR analyses with 2 ng and 0.2 ng template cDNA catalyzed by Normal or Ultralight Pfu DNA polymerase ($n=6$). (D), (E), Comparisons of the corresponding Ct values. (F), Efficiency of PCR with Normal and Ultralight Pfu DNA polymerase ($n=6$). (G), The relative activity of the Ultralight Pfu DNA polymerase compared to Normal enzyme at different temperatures ($n=3$). The plots show mean $\pm$ SEM of experiments. P values were calculated using two-tailed Student's t-test.

The most important finding of this work is that at least some enzymes expressed in *E. coli* grown in the Depleted media show significantly faster kinetics than the identical enzymes produced in the Normal media. This finding is further supported by the faster *E. coli* growth in the Depleted media, which necessitates faster (on average) enzymatic activity in the growing organism. The size of the heavy isotope depletion effect is large (≈ 2.5-fold for luciferase and at least 50% for other enzymes) at normal temperature, with the effect increasing with cooling. It should be noted that the isotope depletion, however large in relative terms (>5-fold), is miniscule in terms of the removed atoms, as the natural abundance of the most abundant depleted isotope, ^{13}C, is only 1.1%. Since only a 13% reduction in the reaction speed of the DHFR enzyme with >90% substituted heavy isotopes of ^{13}C, ^{15}N and ^{2}H at

40°C[22] and a 40% reduction at 5°C[22] were observed, the heuristic expectation of the kinetics enhancement in strictly monoisotopic enzymes is <1%. Thus the kinetics acceleration by up to 250% in Ultralight proteins cannot be accounted by the conventional kinetic isotope effect. The low p-values obtained ($p=3\times10^{-7}$ for luciferase and $p<10^{-11}$ for the combined results of four enzymes) greatly exceed the five-sigma requirement for new discovery accepted in Physics, not to mention the proposed $p<0.005$ threshold for discoveries in Life Sciences.[29] The majority of the Ultralight enzymes are more thermally stable than Normal enzymes (interestingly, the stability of ^{13}C-depleted diamond against 193 nm UV irradiation has also increased[2]), and the superior kinetics of the Ultralight enzymes is preserved even at higher temperatures.
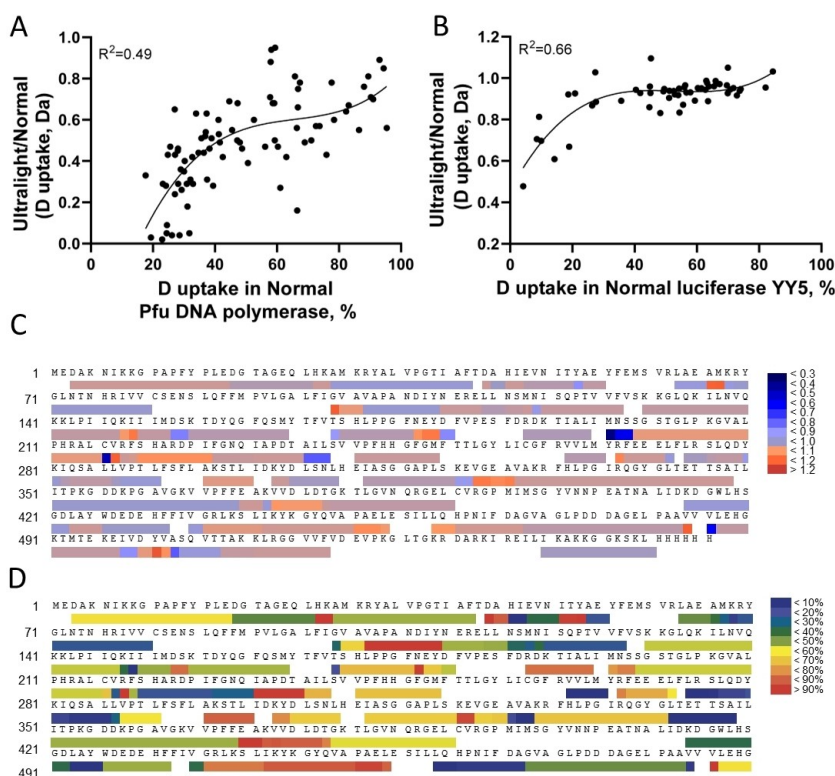
Figure 7. Comparison of deuterium uptake in Ultralight vs Normal Pfu DNA polymerase and luciferase YY5 after 10 min of deuteriation. A, B, Third order polynomial fitting of relative deuterium uptake in Ultralight vs Normal Pfu DNA polymerase ($n = 3$) (A) and in luciferase YY5 frac II ($n = 3$) (B). The peptides with significant difference ($p < 0.1$) in Normal vs Ultralight enzymes were used for this analysis. C, Comparison of deuterium uptake in Ultralight luciferase YY5 frac II compared with Normal enzyme. D, Deuterium uptake in Normal luciferase YY5 frac II.

Mechanistic hypothesis and its testing

As enzymes increase the rates of chemical reaction by up to 10 orders of magnitude compared to uncatalyzed reaction, the acceleration factor of 2–3 observed in the current study may be accounted by minute changes in the active conformation of the enzyme and/or its dynamics. The most plausible hypothesis for the enzyme kinetics acceleration due to isotope depletion seems to be the reduction in conformational and vibrational entropy. Indeed, there are several well-documented cases where the activation free energy decreased due to enzyme's entropic effects by around 10 kcal/mol.[30] The presence of heavy isotopes contributes significantly to the overall protein entropy, with the monoisotopic molecules having the lowest entropy.[31] A single ^{13}C atom in a protein molecule containing 10,000 carbon atoms (as in a ≈ 70 kDa enzyme) will have 10,000 different places to reside in, which immediately results in 10,000 distinct isotopomers. At a 1.1% abundance, there will be on average 110 ^{13}C atoms in such a molecule, giving a very large number of isotopologues[30] differing from each other by the number of ^{13}C atoms. With ^2H, ^{15}N, ^{17}O and ^{18}O isotopes present, each protein isotopologue will have an astronomical number of isotopomers.[32] The electronic structures and the bond strengths of heavy isotopes are slightly different from those of the most abundant light isotopes, which results in a slight distortion of the Ram-

achandran angles in each isotopologue compared to the monoisotopic molecule. As each protein isotopomer has a spectrum of vibrational frequencies distinctly different from other isotopomers,[33] vibrational entropy of a poly-isotopic protein could greatly exceed that of the corresponding monoisotopic molecule or of an Ultralight protein with much fewer heavy isotopes than natural molecule.

Lower vibrational entropy is found to account for the stability of short alpha-helices[34] and to contribute significantly to the stability of globular proteins.[35] Vibrations proximal to the active site are known to play a significant role in the enzymatic activity, with heavy isotopes perturbing the bond vibrations and usually reducing the enzymatic rate.[36] The lower intrinsic entropy due to the isotope depletion can also affect the rates of the protein thermal unfolding and refolding.[37] Furthermore, enzymes such as lactate dehydrogenase, hexokinase, thymidine phosphorylase and purine nucleoside phosphorylase showed surprisingly high isotope effects in binding reactants into catalytic sites.[38] Thus it the ultralight enzymes may be expected to exhibit significantly altered kinetic parameters than the same enzymes with natural isotopic distribution.

One evidence of the entropy difference between the Ultralight and Normal enzymes is the experimentally observed higher melting temperature of ultralight proteins and their steeper melting curves. A change in entropy can move the melting temperature up or down depending upon

the competition between enthalpy and entropy in thermal transition.[39] Also, as the kinetic entropy effects increase with temperature for both Ultralight and Normal enzymes, at higher temperatures the kinetics of both types should converge, and at lower temperatures diverge, in agreement with increasing acceleration factor for Ultralight enzymes at low temperature.

To provide additional experimental support to our hypothesis, we performed hydrogen-deuterium exchange mass spectrometry (HDX MS) analysis of both isotopically depleted and isotopically normal Pfu DNA polymerase. The amide protons from the sites with largest stabilities are the ones most protected from exchange with solvent deuterium, and in such sites the exchange occurs only when the protein molecule acquires a higher-energy conformation via fluctuation in the native state.[40] Therefore, proteins with lower conformation entropy that rarely access such higher-energy conformations should exhibit slower exchange rates in most protected sites and overall. On the other hand, the least protected sites in low-entropy molecules should exhibit elevated exchange rates as deviations from native conformation due to fluctuations can only slow down the exchange rate that is already close to a maximum limit. Our observations on Pfu DNA polymerase agreed with these predictions. While after 24 h in D_2O the average numbers of the protons exchanged to deuterons in 105 pepsin-produced peptides were similar (3.5 and 3.4 in isotopically depleted and normal molecules, respectively, p = 0.63), after a shorter 10 min incubation the isotopically depleted peptides contained on average only 1.0 deuterons versus 1.6 deuterons for the isotopically normal Pfu DNA polymerase ($p < 10^{-4}$, Figure S7, Supporting Information Table 3). The tendency of the sites that exchange slowly in isotopically normal enzyme to exchange even slower in the isotopically depleted molecule and the reverse tendency for the faster exchanging sites was confirmed through the observation of a sigmoidal curve on the corresponding plot (Figure 7A). HDX MS analysis of luciferase YY5 fracII produced qualitatively similar observations (Figure 7B–D, Supporting Information Table 4).

Conclusion

Here we found that isotopically depleted enzymes exhibit significantly faster kinetics than the isotopically normal proteins, with the acceleration factor increasing at lower temperature. A body of observations is in agreement with the lower conformational and vibrational entropy of ultralight enzymes being responsible for the majority of the kinetic acceleration effect. Applications demanding fastest possible reaction rates may benefit from the use of ultralight enzymes.

Acknowledgements

Conflict of Interest

The authors declare no conflict of interest.

Data Availability Statement

The data that support the findings of this study are available in the supplementary material of this article.

[1] T. Ruf, R. W. Henn, M. Asen-Palmer, E. Gmelin, M. Cardona, H. J. Pohl, G. G. Devyatych, P. G. Sennikov, *Solid State Commun.* **2000**, *115*, 243–247.

[2] T. R. Anthony, W. F. Banholzer, J. F. Fleischer, L. Wei, P. K. Kuo, R. L. Thomas, R. W. Pryor, *Phys. Rev. B* **1990**, *42*, 1104–1111.

[3] J. Cline, J. C. Braman, H. H. Hogrefe, *Nucleic Acids Res.* **1996**, *24*, 3546–3551.

[4] J. E. Heidenreich III, M. H. Thiemens, *J. Chem. Phys.* **1986**, *84*, 2129–2136.

[5] a) D. Krankowsky, K. Mauersberger, *Science* **1996**, *274*, 1324–1325; b) G. Michalski, S. K. Bhattacharya, *Proc. Natl. Acad. Sci. USA* **2009**, *106*, 5493–5496.

[6] a) J. J. Katz, H. L. Crespi, R. J. Hasterlik, J. F. Thomson, A. J. Finkel, *J. Natl. Cancer Inst.* **1957**, *18*, 641–659; b) E. Borek, D. Rittenberg, *Proc. Natl. Acad. Sci. USA* **1960**, *46*, 777–782; c) J. J. Katz, H. L. Crespi, *Science* **1966**, *151*, 1187–1194; d) R. A. Uphaus, E. Flaumenhaft, J. J. Katz, *Biochim. Biophys. Acta* **1967**, *141*, 625–632; e) S. Rokop, L. Gajda, S. Parmerter, H. L. Crespi, J. J. Katz, *Biochim. Biophys. Acta Enzymol.* **1969**, *191*, 707–715; f) C. H. Katz JJ, in *Isotope effects in chemical reactions*, Van Nostrand Reinhold, New York, **1971**, pp. 86–363; g) E. B. Fowler, W. H. Adams, C. W. Christenson, V. H. Kollman, J. R. Buchholz, *Biotechnol. Bioeng.* **1972**, *14*, 819–829; h) O. Paliy, D. Bloor, D. Brockwell, P. Gilbert, J. Barber, *J. Appl. Microbiol.* **2003**, *94*, 580–586.

[7] a) G. Somlyai, G. Jancso, G. Jakli, K. Vass, B. Barna, V. Lakics, T. Gaal, *FEBS Lett.* **1993**, *317*, 1–4; b) F. S. Cong, Y. R. Zhang, H. C. Sheng, Z. H. Ao, S. Y. Zhang, J. Y. Wang, *Exp. Ther. Med.* **2010**, *1*, 277–283.

[8] a) A. Kovács, I. Guller, K. Krempels, I. Somlyai, I. Jánosi, Z. Gyomgyi, I. Szabó, I. J. J. o. C. T. Ember, *J. Cancer Ther.* **2011**, *2*, 548–556; b) G. Somlyai, B. Javaheri, H. Davari, Z. Gyöngyi, I. Somlyai, K. A. Tamaddon, L. G. Boros, *Biomacromol. J.* **2016**, *2*, 1–7

[9] X. Zhang, M. Gaetani, A. Chernobrovkin, R. A. Zubarev, *Mol. Cell. Proteomics* **2019**, *18*, 2373–2387.

[10] X. Zhang, J. Wang, R. A. Zubarev, *Mol. Cell. Proteomics* **2020**, *19*, 1790–1804.

[11] a) A. G. Marshall, M. W. Senko, W. Li, M. Li, S. Dillon, S. Guan, T. M. Logan, *J. Am. Chem. Soc.* **1997**, *119*, 433–434; b) K. J. Gallagher, M. Palasser, S. Hughes, C. L. Mackay, D. P. A. Kilgour, D. J. Clarke, *J. Am. Soc. Mass Spectrom.* **2020**, *31*, 700–710.

[12] X. Xie, R. A. Zubarev, *Sci. Rep.* **2015**, *5*, 9215.

[13] a) R. A. Zubarev, K. A. Artemenko, A. R. Zubarev, C. Mayrhofer, H. Yang, Y. M. E. Fung, *Cent. Eur. J. Biol.* **2010**, *5*, 190–196; b) R. A. Zubarev, *Genomics Proteomics Bioinf.* **2011**, *9*, 15–20; c) X. Xie, R. A. Zubarev, *PLoS One* **2017**, *12*, e0169296.

[14] H. Gharibi, A. L. Chernobrovkin, G. Eriksson, A. A. Saei, Z. Timmons, A. C. Kitchener, D. C. Kalthoff, K. Lidén, A. A. Makarov, R. A. Zubarev, *J. Am. Chem. Soc.* **2022**, *144*, 2484–2487.

[15] M. M. Savitski, F. B. M. Reinhard, H. Franken, T. Werner, M. F. Savitski, D. Eberhard, D. M. Molina, R. Jafari, R. B. Dovega, S. Klaeger, B. Kuster, P. Nordlund, M. Bantscheff, G. Drewes, *Science* **2014**, *346*, 1255784.

[16] A. A. Saei, C. M. Beusch, P. Sabatier, J. A. Wells, H. Gharibi, Z. Meng, A. Chernobrovkin, S. Rodin, K. Näreoja, A. G. Thorsell, T. Karlberg, Q. Cheng, S. L. Lundström, M. Gaetani, Á. Végvári, E. S. J. Arnér, H. Schüler, R. A. Zubarev, *Nat. Commun.* **2021**, *12*, 1296.

[17] T. Pozzo, F. Akter, Y. Nomura, A. Y. Louie, Y. Yokobayashi, *ACS Omega* **2018**, *3*, 2628–2633.

[18] G. A. Khoury, R. C. Baliban, C. A. Floudas, *Sci. Rep.* **2011**, *1*, 90.

[19] R. A. Zubarev, P. A. Demirev, P. Haakansson, B. U. R. Sundqvist, *Anal. Chem.* **1995**, *67*, 3793–3798.

[20] E. S. Arnér, A. Holmgren, *Eur. J. Biochem.* **2000**, *267*, 6102–6109.

[21] H. Lodish, A. Berk, S. L. Zipursky, P. Matsudaira, D. Baltimore, J. Darnell, in *Molecular Cell Biology*, WH Freeman, New York, **2000**, pp. 37–46.

[22] L. Y. P. Luk, J. J. Ruiz-Pernía, W. M. Dawson, E. J. Loveridge, I. Tuñón, V. Moliner, R. K. Allemann, *J. Am. Chem. Soc.* **2014**, *136*, 17317–17323.

[23] R. A. Bender, D. M. Makula, *Br. J. Cancer* **1978**, *37*, 403–410.

[24] S. Paik, C.-y. Kim, Y.-k. Song, W.-s. Kim, *Nat. Clin. Pract. Oncol.* **2005**, *2*, 246–254.

[25] B. D. Kevadiya, J. Machhi, J. Herskovitz, M. D. Oleynikov, W. R. Blomberg, N. Bajwa, D. Soni, S. Das, M. Hasan, M. Patel, A. M. Senan, S. Gorantla, J. McMillan, B. Edagwa, R. Eisenberg, C. B. Gurumurthy, S. P. M. Reid, C. Punyadeera, L. Chang, H. E. Gendelman, *Nat. Mater.* **2021**, *20*, 593–605.

[26] S. Ishino, Y. Ishino, *Front. Microbiol.* **2014**, *5*, 465–465.

[27] Y. Wang, D. E. Prosen, L. Mei, J. C. Sullivan, M. Finney, P. B. Vander Horn, *Nucleic Acids Res.* **2004**, *32*, 1197–1207.

[28] J. Huggett, K. Dheda, S. Bustin, A. Zumla, *Genes Immun.* **2005**, *6*, 279–284.

[29] D. J. Benjamin, J. O. Berger, M. Johannesson, B. A. Nosek, E. J. Wagenmakers, R. Berk, K. A. Bollen, B. Brembs, L. Brown, C. Camerer, D. Cesarini, C. D. Chambers, M. Clyde, T. D. Cook, P. De Boeck, Z. Dienes, A. Dreber, K. Easwaran, C. Efferson, E. Fehr, F. Fidler, A. P. Field, M. Forster, E. I. George, R. Gonzalez, S. Goodman, E. Green, D. P. Green, A. G. Greenwald, J. D. Hadfield, L. V. Hedges, L. Held, T. Hua Ho, H. Hoijtink, D. J. Hruschka, K. Imai, G. Imbens, J. P. A. Ioannidis, M. Jeon, J. H. Jones, M. Kirchler, D. Laibson, J. List, R. Little, A. Lupia, E. Machery, S. E. Maxwell, M. McCarthy, D. A. Moore, S. L. Morgan, M. Munafó, S. Nakagawa, B. Nyhan, T. H. Parker, L. Pericchi, M. Perugini, J. Rouder, J. Rousseau, V. Savalei, F. D. Schönbrodt, T. Sellke, B. Sinclair, D. Tingley, T. Van Zandt, S. Vazire, D. J. Watts, C. Winship, R. L. Wolpert, Y. Xie, C. Young, J. Zinman, V. E. Johnson, *Nat. Hum. Behav.* **2018**, *2*, 6–10.

[30] J. Åqvist, M. Kazemi, G. V. Isaksen, B. O. Brandsdal, *Acc. Chem. Res.* **2017**, *50*, 199–207.

[31] P. Dittwald, D. Valkenborg, J. Claesen, A. L. Rockwood, A. Gambin, *J. Am. Soc. Mass Spectrom.* **2015**, *26*, 1732–1745.

[32] J. Yergey, D. Heller, G. Hansen, R. J. Cotter, C. Fenselau, *Anal. Chem.* **1983**, *55*, 353–356.

[33] J. W. Brauner, C. Dugan, R. Mendelsohn, *J. Am. Chem. Soc.* **2000**, *122*, 677–683.

[34] M. Rossi, M. Scheffler, V. Blum, *J. Phys. Chem. B* **2013**, *117*, 5574–5584.

[35] M. Goethe, I. Fita, J. M. Rubi, *J. Chem. Theory Comput.* **2015**, *11*, 351–359.

[36] I. Zoi, J. Suarez, D. Antoniou, S. A. Cameron, V. L. Schramm, S. D. Schwartz, *J. Am. Chem. Soc.* **2016**, *138*, 3403–3409.

[37] O. V. Galzitskaya, *Entropy* **2010**, *12*, 961–982.

[38] V. L. Schramm, *Curr. Opin. Chem. Biol.* **2007**, *11*, 529–536.

[39] M. B. Jackson, in *Molecular and cellular biophysics*, Cambridge University Press, New York, **2006**, pp. 5–12.

[40] B. M. Huyghues-Despointes, C. N. Pace, S. W. Englander, J. M. Scholtz, *Methods Mol. Biol.* **2001**, *168*, 69–92.